

Spatiotemporal dynamics of an intrinsically chaotic field

Farid F. Abraham

IBM Research Division, Almaden Research Center, 650 Harry Road, San Jose, California 95120-6099

(Received 5 October 1992)

In contrast to earlier nonlinear-dynamics investigations concerning the consequences of coupling limit-cycle oscillators, we propose the conceptionally simple extension of studying the interaction dynamics of chaotic subsystems. We illustrate this by simulating a “toy system,” the dynamics of a linear chain of damped-driven pendulums where the state of the isolated individual pendulum is chaotic. The harmonic coupling between these chaotic oscillators results in a very complex and rich spatiotemporal dynamics as a function of coupling strength and system size. This suggests that the extension to realistic representations of physical systems may provide a fruitful paradigm for studying dynamical disorder in the real world.

PACS number(s): 05.45.+b

A one-dimensional (1D) chain of interacting point particles is a paradigm from which we learned about certain limited dynamical behavior occurring in many-body systems. From this idealized model has evolved a more general picture of a dynamical system defined by an assembly of a large number of identical subsystems of known intrinsic dynamics which are coupled to each other in some specific manner [1,2]. The general goal is to study the global dynamical behavior of the total system on the basis of the known nature of the subsystem and the coupling between a large number of subsystems. An example would be a chemical solution of some oscillating reaction where the total system is imagined as forming a diffusion coupled field of similar limit-cycle chemical oscillators [3,4].

We now introduce a further generalization of this synthetic view of a dynamical system by allowing a much richer intrinsic behavior of the elementary subsystem; in particular, we consider the dynamics of the “independent” subsystem to be chaotic, instead of a simpler limit-cycle oscillation. Through intersubsystem coupling, the individual subsystem dynamics may change dramatically in both space and time. In terms of a linear chain of atoms, we replace the atom by a chaotic oscillator, or an “atom” with an internal chaotic state when in isolation. It is the interatomic coupling between these “chaotic atoms” that gives rise to a very complex and rich spatial-temporal many-body dynamics as a function of coupling strength. Of course, we are not limited to chaotic oscillators, coupled harmonically, and ordered linearly.

Ruelle, in his book entitled *Chance and Chaos*, points out that most approximate theories of fluid turbulence assume that turbulence is homogeneous while turbulence is actually spatially and temporally inhomogeneous with the coexistence of fluctuating regions of smooth and erratic dynamics [5]: “In reality, a turbulent fluid always shows clumps of intense turbulence in a relatively quiescent background. And hydrodynamicists keep looking for the correct theory to describe this clumpiness.” This observation provided the motivation to think of a coarse-grain model of a system where each subsystem is

“turbulent” in isolation and to study the total system dynamics arising from intersubsystem coupling; i.e., does the intrinsic “homogeneous turbulence” of the collective subcells give rise to a global dynamical structure that is not uniformly turbulent in space and time?

For our “toy system” of a linear chain of chaotic oscillators, we take the chaotic oscillator, or active subsystem, to be the damped-driven pendulum [6]. Of course, this is not meant to model a turbulent system. This simple nonlinear mechanical system is the familiar pendulum with the additional features of a linear damping term proportional to its angular velocity and a driving oscillatory torque. The angle the pendulum makes with the vertical is denoted by ϕ , α is the damping factor, ω_0 is the natural frequency of the simple pendulum, and ω and A are the frequency and amplitude of the external torque. The dynamical equation is a second-order differential equation,

$$\frac{d^2\phi}{dt^2} = -\alpha \frac{d\phi}{dt} - \omega_0^2 \sin(\phi) + A \cos(\omega t). \quad (1)$$

This subsystem can operate in far-from-equilibrium situations so that it represents a very active functional subunit of the total system. We choose the following values for the parameter which gives a chaotic state of the isolated pendulum: $\omega_0 = 2.53$, $\alpha = 0.25$, $\omega = 1.62$, $A = 3.8$. These parameters are not changed in our study.

Our total dynamical system is a linear chain of these chaotic pendulums coupled harmonically in ϕ with a coupling constant κ . The force $F_\kappa(k)$ on the k th pendulum due to the neighboring pendulums is

$$F_\kappa(k) = \kappa[\phi(k+1) + \phi(k-1) - 2\phi(k)]. \quad (2)$$

We have studied the system dynamics of this linear chain of chaotic pendulums as a function of chain length N (or number of pendulums) and coupling constant κ . The initial angles and velocities are taken to be random, and periodic boundary conditions are imposed between the two end pendulums. However, we note two obvious dynamical features of this system: for $\kappa = 0$, we have N

independent chaotic oscillators, and for $\kappa \gg 1$, we have one “large” chaotic oscillator. We are interested in discovering what is between zero coupling and infinite coupling; hence the many-body physics of chaotic oscillators. It is obvious that harmonic coupling is a very primitive coupling scheme. For examples of more complex coupling models (as applied to limit-cycle oscillators), we refer the reader to the study by Daido [4]. Questioning whether phenomena in coupled map lattice systems are really indicative of typical phenomena in systems that are continuous in time and space, Umberger, Grebogi, Ott, and Afeyan [7] studied a one-dimensional chain of Duffing oscillators as a function of driving amplitude. This pioneering approach showed that chaotic transit behavior became longer as the driving amplitude increased until the time dependence apparently correspond to sustained chaos.

We use a special feature of one-dimensional systems which distinguishes them from multidimensional systems. Having the atoms arranged along a single coordinate, we can treat “time” as the second Cartesian axis. So we can trace the vibrations for each pendulum in time like a multipen strip-chart recorder where each pen’s average position corresponds to the 1D atomic lattice position of a vertically oriented chain. Instead of tracing the continuous evolution of the vibrations, we record the discrete positions from a Poincaré section, but connect them with straight-line segments. This mathematical technique simplifies the complicated dynamics and is constructed by viewing the trajectory stroboscopically in such a way that the motion is observed periodically. The strobe period is equal to the forcing period of the individual pendulums and is the same for all of the pendulums. For periodic motion, there are a finite number of points in the Poincaré section where the motion continues to return, and our picture will show a saw-tooth trajectory with that return period. For chaotic motion, the trajectory will be “noisy” with no periodicity. We choose the velocity from the Poincaré point in generating the stroboscopic trajectory. If we take position, our plots could deviate from average straight-line behavior due to “kinks” resulting from complete revolutions about the pivot of an individual pendulum. We also made Poincaré plots for individual oscillators. This was not as useful because the analysis implies “a constancy of dynamical behavior” during the sampling interval, a condition likely to be violated for a particular simulation unless prior knowledge of the dynamics was available.

In Fig. 1, a simplistic description of the general dynamics of our model is presented where three types of behavior are loosely identified (periodic, chaotic, and mixed) as a function of system size N (the number of pendulums) and the coupling constant κ . For periodic behavior, all of the pendulums are oscillating with a Poincaré periodicity P_n , where n is the period return number. In our study, we have seen only $n = 1$ and 3. The chaotic behavior is characterized by a variety of the spatiotemporal patterns that will be described later. The mixed region is composed of periodic and chaotic regions (depending on the coupling) that we choose to associate only with the system of size N since we could not

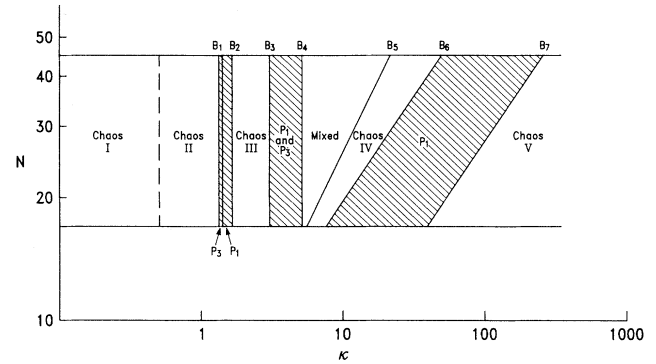


FIG. 1. The “phase diagram” of the general dynamics of our model is presented where three types of behavior are qualitatively identified (periodic, chaotic, and mixed) as a function of system size N (the number of pendulums) and the coupling constant κ .

identify any common dynamical features in this regime among the different systems that we studied ($N = 18, 27, 36, 45$). The simplest identifications were for regions that have no size dependence in the dynamical behavior which is the case for $\kappa < 5$ (the boundaries B_n between the various dynamical regions in Fig. 1 are vertical).

In Fig. 1, the dynamics is labeled as chaos I for $0 < \kappa < 0.5$ and chaos II for $0.5 < \kappa < 1.3$. The strobos-

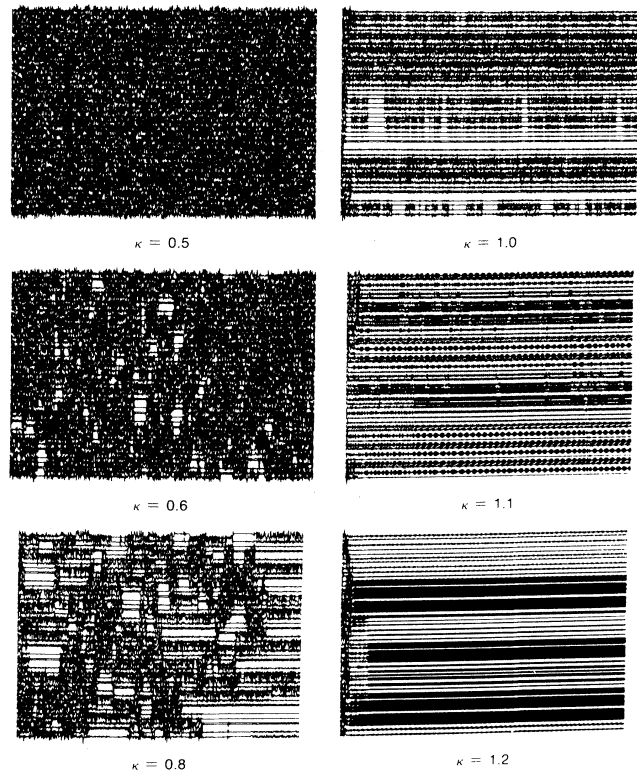


FIG. 2. The stroboscopic space-time trajectories for the model system with $N = 45$ and for κ passing through the chaos-II regime as identified in Fig. 1.

scopic space-time (SST) trajectories for the system with $N=45$ and for κ passing through the transition chaos-II regime are shown in Fig. 2. The trajectories for chaos I are much the same as for $\kappa=0.5$ in Fig. 2. However, for chaos II the character, or “texture,” of the SST plot changes rapidly as κ increases toward 1.3. At $\kappa=0.6$, we see vertically elongated holes in the space-time fabric representing relatively quiescent dynamics among a few nearest-neighbor pendulums and these holes appear to occur intermittently in time. With increasing κ patches of quiescent dynamics elongate along the time axis, and the amplitudes of the chaotic noise decrease, eventually giving the appearance of fuzzy, worn threads of varying thickness as time evolves ($\kappa=1.0$). At $\kappa=1.1$, the patterns along each time string are bizarre, many having resonating balls of chaotic noise with a quasiperiodic appearance. P_3 dynamics occurs at $\kappa=1.3$.

Passing through P_3 to P_1 dynamics, we enter the chaos-III region bounded by $1.6(4) < \kappa < 3.0$. In Fig. 3, we see the chaotic bands traversing the space-time area leaving patches of periodic or low noise regions, these patches decreasing in size with increasing coupling until chaos completely dominates for $2.0 < \kappa < 3.0$. In Fig. 4, the superposition of ten consecutive snapshot configurations is shown for $N=45$ and for $\kappa=1.64$ at times 200–1000 and using the driven period as the time-step interval. Note the traveling wave of chaotic behavior. From $3.0 < \kappa < 4.0$, we observe a mixture of P_1 and P_3 , and for $4.0 < \kappa < 5.0$ we observe P_1 .

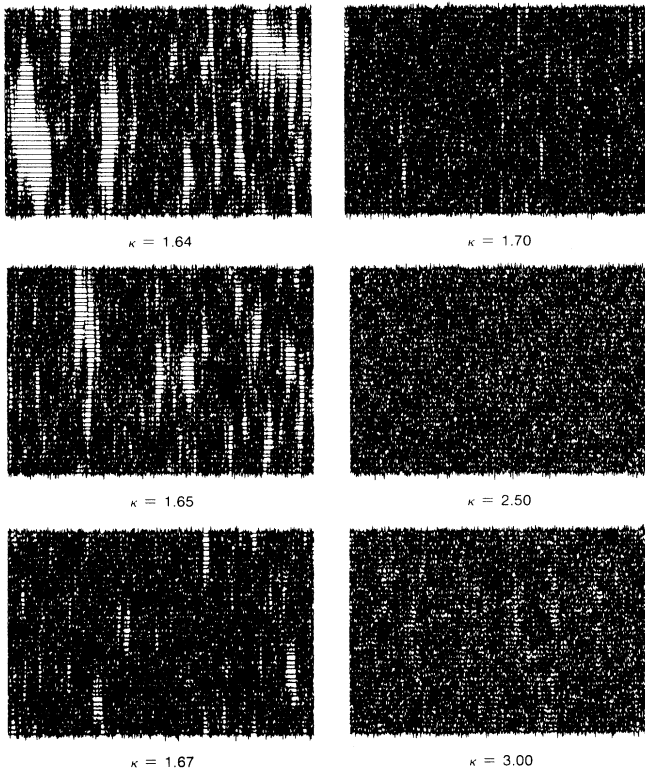


FIG. 3. The stroboscopic space-time trajectories for the model system with $N=45$ and for κ passing through the transition chaos-III regime as identified in Fig. 1.

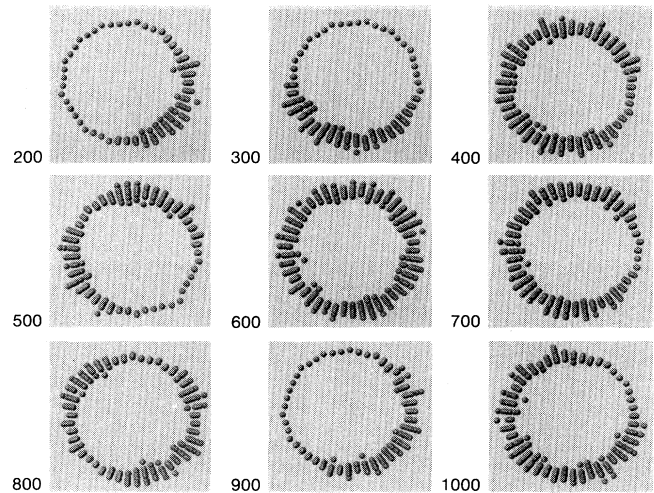


FIG. 4. The superposition of ten consecutive snapshot configurations for our model system with $N=45$ and for $\kappa=1.64$ at times 200–1000 and using the driven period as the time-step interval. Note that the pendulum is depicted as a ball, hence the overlap of ball images with chaotic motion.

In Fig. 5, for the chaos-IV region, the texture of the ST plot changes smoothly as κ increases from 23.0. We see vertical stripe bands in the space-time fabric representing relatively quiescent (low noise) dynamics among the entire chain and these stripes appear to occur intermittently in time. With increased coupling the stripes of quiescent dynamics diminish in frequency until the field is solely chaotic dynamics. When the B_6 boundary is reached, the dynamics becomes P_1 and remains P_1 until B_7 is reached by increasing κ . For the chaos-V region, the ST plot is much like the chaos-IV region except that the stripes are much less noisy because of the greater coupling. Extreme coupling leads to the limit of all of the pendulums vibrating like a single damped-drive pendulum.

For sufficiently large couplings, the phase diagram has periodic and chaotic regions (depending on the magnitude of the coupling) that scale with the system size N ; e.g., we believe that we have identified common dynamical features in these scaling regimes for the different sizes studied ($N=18, 27, 36, 45$). The boundaries B_5 , B_6 , and B_7 defining the scaling regions in Fig. 1 are slanted with the slope giving the power-law dependence of the boundaries with size N . The κ points defining boundary B_5 scale as $N^{3/2}$, while B_6 and B_7 scale as N^2 . The dynamical behavior scaling with N^2 as κ becomes large can be understood by approximating our dynamical equations by the partial differential equation,

$$\frac{\partial^2 \phi}{\partial t^2} = \beta \frac{\partial^2 \phi}{\partial x^2} - \alpha \frac{\partial \phi}{\partial t} - \omega_0^2 \sin(\phi) + A \cos(\omega t), \quad (3)$$

where $\beta = a^2 \kappa$ and a is the lattice spacing in approximating Eq. (2) by a second-order partial derivative. If the characteristic features of the dynamics scale with the length of the chain $L = aN$, then from Eq. (3) we conclude that $\beta/L^2 = a/L^2 \kappa = \text{const}$. Therefore, the scale-

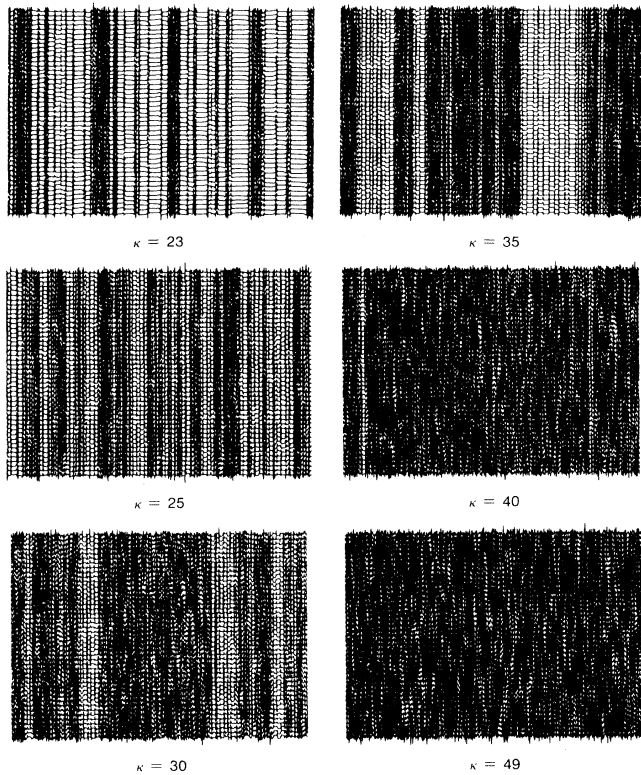


FIG. 5. The stroboscopic trajectories for our model system with $N=45$ and for κ passing through the chaos-IV regime as identified in Fig. 1.

invariant dynamics satisfies the relation $\kappa = \text{const} \times N^2$. Scale invariance is what is expected in the limit of strong coupling where the motion between oscillators is forced to be in concert.

Because the innermost slant boundary B_5 intersects with the outermost vertical boundary B_4 at approximately $N=15$, we see a wedge-shape region expanding with system size N with dynamics not accounted for by the

TABLE I. Dynamical behavior as a function of system size N and coupling strength κ for the “mixed” region.

κ	6	7	8	9	10	11	12	13	14	15	16	17	18	19	20	21	22
N																	
45	C	C	C	P_1	P_1	C	C	C	C	P_1	P_1	C	P_1	P_1	P_1	P_1	P_1
36	C	C	C	C	C	P_1	P_1	P_1	C	P_1							
27	P_1	P_1	P_1	P_1	P_3												

size-invariant regions and the scaling regions bounding the wedge. Possibly new scaling regions exist but cannot be determined because of the limited finite-size span of this study. We list in Table I what we observed for each system size.

We have learned that this simple model of coupled, “intrinsically” chaotic subsystems can exhibit a very rich and complex dynamics, both in space and time. Of course, the obvious is to study larger systems, different types of chaotic subsystems, various local and nonlocal coupling schemes, higher-dimension packings, mixed systems (chaotic and periodic subsystems), frustration and much more. For example, Haken has shown that the Lorenz model of fluid convection is identical with the model of a single-mode laser (8). If, in Haken’s equations (7)–(9), the gradient of the electric field is not equated to zero, we have a partial differential equation that, upon finite differencing in space, gives rise to a set of coupled ordinary differential equations. At each lattice point, we have the Lorenz equations for the discretized state variables which are coupled to neighboring lattice points by the field gradient. In the spirit of our study, one would choose Lorenz parameters to describe chaos and investigate the laser dynamics for increasing field gradients.

However, the very simple concept of modeling the interaction of chaotic subsystems may provide a new paradigm for studying spatiotemporal chaos in the real world.

The author thanks Dr. Mark Goulian (UCSB) for stimulating conversations and for bringing Ref. [3] to his attention.

- [1] R. Z. Sagdeev, D. A. Usikov, and G. M. Zaslavsky, *Nonlinear Physics: From the Pendulum to Turbulence* (Harwood, Academic, Chur, Switzerland, 1988).
- [2] E. Atlee Jackson, *Perspectives of Nonlinear Dynamics: I and II* (Cambridge University Press, Cambridge, England, 1991).
- [3] Y. Kuramoto, *Chemical Oscillations, Waves, and Turbulence* (Springer-Verlag, Berlin, 1984).
- [4] H. Daido, Phys. Rev. Lett. **68**, 1073 (1992). Especially, see Ref. [2] therein for further references on model systems of

- coupled limit-cycle oscillators.
- [5] D. Ruelle, *Chance and Chaos* (Princeton University, Princeton, NJ, 1991).
- [6] G. L. Baker and J. P. Gollub, *Chaotic Dynamics: An Introduction* (Cambridge University Press, Cambridge, England, 1990).
- [7] D. K. Umberger, C. Grebogi, E. Ott, and B. Afeyan, Phys. Rev. A **39**, 4835 (1989).
- [8] H. Haken, Phys. Lett. **53A**, 77 (1975).

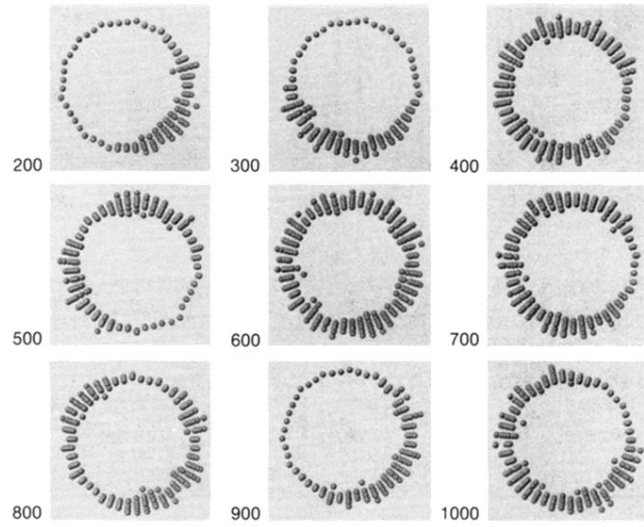


FIG. 4. The superposition of ten consecutive snapshot configurations for our model system with $N=45$ and for $\kappa=1.64$ at times 200–1000 using the driving period as the time-step interval. Note that the pendulum is depicted as a ball, hence the overlap of ball images with chaotic motion.